Time scale of entropic segregation of flexible polymers in confinement: Implications for chromosome segregation in filamentous bacteria

Axel Arnold*

FOM-Institute AMOLF, Kruislaan 407, 1098 SJ Amsterdam, The Netherlands

Suckjoon Jun†

Faculté de Médecine, INSERM Site Necker, U571, 156 rue de Vaugirard, 75015 Paris, France

We report molecular dynamics simulations of the segregation of two overlapping chains in cylindrical confinement. We find that the entropic repulsion between chains can be sufficiently strong to cause segregation on a time scale that is short compared to the one for diffusion. This result implies that entropic driving forces are sufficiently strong to cause rapid bacterial chromosome segregation.

I. INTRODUCTION

Confined polymers play an important role in many industrial processes and biological systems. Examples range from membrane filtration and oil recovery to gel electrophoresis and protein translocation [1–3]. Importantly, recent technological development in nanofluidics and microfluidics has made it possible to manipulate and trap biomolecules such as double-stranded (ds) DNA in confined environments with a characteristic length scale that is much smaller than the radius of gyration of the polymers [4–6]. Also, under biological conditions, DNA is often strongly confined—e.g., packed into a viral capsid [7], bacteria [8], or the eukaryotic cell nucleus [9].

In this article, we report molecular dynamics (MD) simulations that allow us to determine the typical speed of the segregation of initially mixed polymers in cylindrical confinement. This problem has particular relevance for the understanding of chromosome segregation in bacteria, where the nature of its underlying mechanism is currently under debate. Here, the basic issue is whether the major driving force for the segregation of duplicating chromosomes in strong confinement is physical (driven by entropy or mechanical "pushing") [8,10] or biological (such as cytoskeletal and motor proteins) [11,12].

Our results show that the effective repulsion between two chains in a cylindrical geometry of confinement can be very strong. Typically, the segregation requires a time proportional to N^2, which is much faster than the N^3 time scale of chain diffusion, where N is the chain length. This suggests that for filamentous bacteria such as *Streptomyces coelicolor* [13] or cyanobacterium *Anabaena* [14], the main driving force of chromosome segregation might be entropic and any additional mechanisms are for "optimization." As we shall discuss later, our proposal is fully consistent with the recent results that chromosome segregation in some filamentous bacteria is a *random* process [14].

---

*arnold@amolf.nl

†Present address: FAS Center for Systems Biology, Harvard University, Cambridge, MA 02138, USA.

II. THEORY

Consider two linear chains with excluded-volume interactions, which are initially intermingled and confined in an infinitely long cylinder with a diameter D that is much smaller than the radius of gyration, R_g, of the unconfined chains (Fig. 1). As the two chains can gain conformational entropy by demixing, they effectively repel each other. Note that the free-energy cost for simultaneous overlap of n chains scales as $n^{9/4}$ in the dilute regime and then increases faster as n^3 in the more concentrated regime, independent of the chain length [15,16]. Thus, for the two intermingling chains illustrated in Fig. 1, each blob-blob overlap contributes $\sim k_B T$ ($n=2$) to the free-energy cost. The potential of mean force for segregation between the two chains then is proportional to the total number of overlapping blobs—i.e., $\beta \mathcal{F}(R_{c2c}) \simeq (L_{eq} - R_{c2c})/D$, where L_{eq} is the equilibrium length of an isolated individual chain in the pore and R_{c2c} the center-to-center distance between the two chains. The effective repulsive force is then obtained as

$$F_{\text{eff}} = -\frac{\partial \mathcal{F}}{\partial R_{c2c}} = \frac{k_B T}{D}, \tag{1}$$

and, thus, the equation of motion for the center of mass is

$$M \dot{V}_{c2c} = \frac{k_B T}{D} - \Gamma V_{c2c}, \tag{2}$$

where $M = Nm$ and Γ are the total mass and the effective friction of the chain, respectively (m is the mass of a single monomer). Ignoring hydrodynamic interactions between
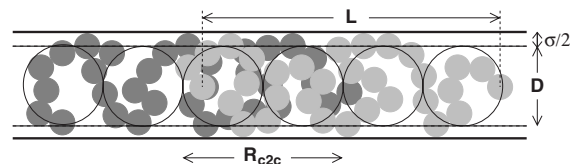

FIG. 1. Two partly overlapping chains in a spherical cylinder of width D. The chains consist of N beads of size σ each. L denotes the chain extension and R_{c2c} the distance of the centers of mass.

monomers, one can assume that the frictions γ on the individual monomers are additive—i.e., also $\Gamma = N\gamma$. Then, the solution of Eq. (2) with an initial condition $V_{\text{c2c}} = 0$ at $t = 0$ can be obtained as

$$V_{\text{c2c}}(t) = \frac{k_B T}{\gamma D N}(1 - e^{-t/\tau^*}), \qquad (3)$$

where $\tau^* = m/\gamma$ is the "inertial" time scale. In practice, $t \gg \tau^*$ and hence the characteristic segregation speed is constant and given by

$$V_{c2c} \sim \frac{k_B T}{\gamma D N}. \qquad (4)$$

The equilibrium length of confined chains, L_{eq}, is proportional to N. Therefore, the time for reaching complete segregation, $R_{\text{c2c}} = L_{\text{eq}}$, scales as

$$t_s \sim L_{\text{eq}}/V_{\text{c2c}} \sim N^2. \qquad (5)$$

This time is much shorter than t_{diff}, the typical time it takes a single chain to diffuse over a distance equal to its own length:

$$t_{\text{diff}} \sim \frac{L_{\text{eq}}^2}{2D_{\text{diff}}} \sim N^3. \qquad (6)$$

However, the above considerations do apply for the initial situation of complete overlap, $R_{\text{c2c}} \approx 0$. In this case the system is in a state of unstable equilibrium, since the effective segregation force is $F_{\text{eff}} \approx 0$. Hence, the system will initially show purely diffusive behavior until a certain separation, typically $R_{\text{c2c}} \approx D$, is reached. We refer to the time until segregation sets in as the "induction time" t_i that should scale as N^3. With increasing D, diffusion becomes easier, because the monomer concentration decreases and t_i decreases, while t_s increases with D. Below, we show that for all practically relevant diameters, the segregation process is rate limiting.

For real bacteria, entropic segregation already sets in during replication. Therefore, segregation always takes place for comparatively short pieces of DNA, so that the induction time does not play a role.

III. SIMULATION METHOD

In the molecular dynamics simulations, we model the polymers using a bead-spring model in a cylindrical compartment of diameter D; each chain consists of N beads of diameter σ. The bead-bead and bead-compartment interactions were modeled by a Weeks-Chandler-Andersen (WCA) potential [17], which corresponds to the repulsive part of the Lennard-Jones potential:

$$U_{\text{WCA}}(r) = \epsilon_{\text{WCA}}\left[\left(\frac{\sigma}{r}\right)^{12} - \left(\frac{\sigma}{r}\right)^6 + \frac{1}{4}\right] \qquad (7)$$

for $r < \sqrt[6]{2}\sigma$ and 0 elsewhere. r denotes the distance between two bead centers for the bead-bead interactions and the distance between the bead center and the compartment minus σ for the bead-compartment interactions. At $r = \sigma$, the interaction energy is $\epsilon_{\text{WCA}} = 1k_B T$; since the potential is quite steep,

r will typically stay above 0.9σ. This models soft beads of diameter σ, whose centers cannot come much closer than σ to each other and cannot penetrate the wall (i.e., the wall imposes a constraint on the sphere centers, as depicted in Fig. 1). In the simulation, σ defines the basic length scale and ϵ_{WCA} the energy scale. Our unit of mass is given by m, the mass of a bead. We choose the temperature such that $k_B T/\epsilon = 1$. Having specified our basic units, the time unit is given by $\tau_{\text{WCA}} = \sigma\sqrt{m/\epsilon_{\text{WCA}}} = 1$. In the following, we will omit these units.

The springs between the beads in a chain were formed by the finite extensible nonlinear elastic (FENE) potential

$$U_F(r) = -\frac{1}{2}\epsilon_F r_F^2 \ln\left[1 - \left(\frac{r}{r_F}\right)^2\right], \qquad (8)$$

where r is the distance of the bead centers, r_F is the radius at which the potential becomes singular, and ϵ_F is the interaction strength. In the present simulations, we chose $\epsilon_F = 10$ and $r_F = 2$. In combination with the WCA potential this results in a typical bond length of 1.027.

We simulate this system using the simulation package ESPResSo [18]. To propagate the system, we employ a velocity-Verlet MD integrator with a fixed time step of 0.01; the system is kept at constant temperature by means of a Langevin thermostat with a fixed friction of $\gamma = m\tau_{\text{WCA}}^{-1}$, so that $\tau^* = \tau_{\text{WCA}} = 1$. Other parameters vary for the different simulation runs; see Table I. Our simulation procedure contains four steps:

The system is initially prepared in a "ladder" configuration formed by two interconnected zigzag strands; i.e., the system consists of two linear chains where the ith bead of one chain is bonded to the ith bead of the other chain, in addition to the bonds to its neighbors within the same chain.

To equilibrate the system, we simulate for T_{warm} steps with a "soft" WCA potential—i.e., a WCA potential that has been modified such that the potential is linear for distances smaller than a radius r_{fc}. We reduce r_{fc} gradually during the equilibration phase, so that the potential converges to the plain WCA interaction. This procedure allows more overlap between beads during the initial equilibration phase, which helps the bonds to quickly relax to the equilibrium length.

After the equilibration of the interconnected chains, we remove the interconnecting bonds to obtain two separate chains whose centers of mass very nearly coincide. The chains are stretched by about 10%–20% compared to a single chain in confinement due to the cross-linking; however, their length relaxes quickly to almost the same length as a single chain once the cross-linking is released. The time scale for this relaxation is negligible compared to the segregation time.

We continue to simulate the system until the two chains have segregated—i.e., until the chains do not overlap and their centers of mass are separated by at least the equilibrium length L_{eq} of a single chain, which had been determined beforehand by separate simulations. During this run, we record configurations every T_{config} simulation steps.

This procedure is repeated N_{config} times (see Table I), resulting in N_{config} independent data sets similar to Fig. 2. For

TABLE I. The simulation parameters for the different runs. The first six rows give for different chain lengths N the simulated pore diameters D and the corresponding equilibrium end-to-end distances L_{eq} of a single chain. The last three rows contain the number T_{warm} of time steps used for equilibration of the interconnected chains, the number of time steps T_{config} between recorded configurations, and the number N_{config} of independent simulations runs with different random seeds.

$N=100$	D	1.5	2	2.5	3	4	5			
	L_{eq}	72.5	64.4	58.1	52.8	44.2	37.6			
$N=200$	D	1.5	2	2.5	3	4	5	7	9	
	L_{eq}	146.0	130.3	118.0	107.6	91.2	78.9	61.1	49.4	
$N=300$	D	2	3	4	5	6	7	8	9	11	13
	L_{eq}	190.4	162.1	133.2	121.2	105.2	94.6	88.2	77.6	64.8	55.8

N	T_{warm}	T_{config}	N_{config}	N	T_{warm}	T_{config}	N_{config}
100	10^5	2000	800	300	1.8×10^6	36000	200
200	8×10^5	8000	1000				

each of these data sets, we calculate the distance $R_{c2c}(t)$ of the centers of mass of the two chains parallel to the cylindrical compartment as a function of time. Initially, R_{c2c} is zero due to the preparation of the system and stays close to zero during the induction time. Eventually, segregation sets in and R_{c2c} grows rapidly until $R_{c2c}=L_{eq}$ is reached, at which time the chains do not overlap anymore. Further increase in R_{c2c} is only due to diffusion and is therefore much slower.

Figure 3 displays schematically how we extract the induction and segregation times from each run: we fit a linear function $(t-t_i)V_{c2c}$ to the range in which $R_{c2c}(t)$ is between D and $L_{eq}-D$. Here, t_i is the extrapolated onset time of segregation and V_{c2c} is the speed with which the two centers of mass separate in the linear regime. We always find linear segregation behavior for $D\leqslant R_{c2c}\leqslant L_{eq}-D$. The lower limit implies that the chains are separated by at least one blob diameter; the upper limit guarantees that there is at least one blob-size overlap left.
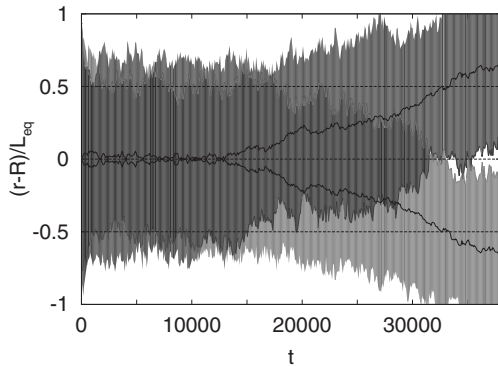

FIG. 2. Example simulation run for $D=7$, $N=200$, starting from the removal of the interconnecting bonds. The two gray bands give the total extent along the tube axis of the two chains for a single run, the black lines the positions of their centers of masses. The positions are relative to the total center of mass, R, of the system and rescaled by the equilibrium length L_{eq} of a single confined chain.

IV. RESULTS AND DISCUSSION

As can be seen in Fig. 4, our simulation clearly support the scaling prediction $V_{c2c}\sim 1/(ND)$ [Eq. (4)]. The prediction that the segregation time scales as N^2 is only recovered for small tube diameters. This is not unexpected, because when D approaches L_{eq}, the simple blob prediction for L_{eq} breaks down [19] and the segregation time levels off at the relaxation of a free chain. The segregation speed relation, Eq. (4), however, seems to be quite robust even for finite systems.

The measured average induction time t_i is shown in Fig. 5. The distribution of the induction times has a long tail, which makes it difficult to sample t_i accurately. Keeping this caveat in mind, we find that for small tube diameters the t_i's computed for different chain lengths can be made to collapse if we assume N^3 scaling, as expected for a diffusive process. Moreover, we do observe the expected decrease of t_i with increasing D. For larger tube diameters, the induction time increases again; this is probably due to the fact that for larger D the segregation and induction times cannot be clearly separated $[t_i/t_s=\mathcal{O}(1)]$ for larger diameters. In fact, in our
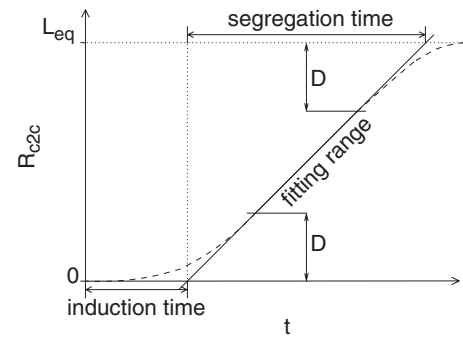

FIG. 3. Schematic view of the segregation process. A line is fitted to the center-of-mass distance R_{c2c} in the range from D to $L_{eq}-D$. From this fit, the induction time t_i is determined as intersection with $R_{c2c}=0$ and the segregation speed V_{c2c} as its slope. The segregation time is then $t_s=L_{eq}/V_{c2c}$.
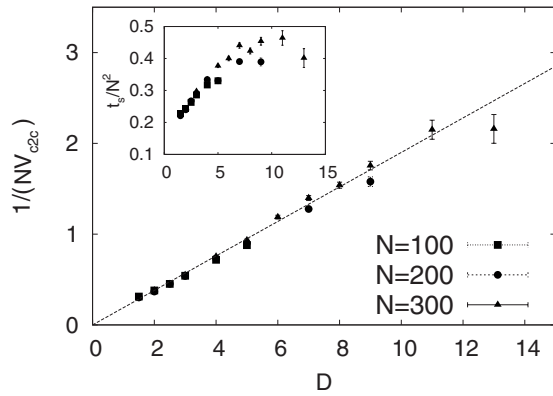
FIG. 4. Measured segregation speed V_{c2c} rescaled by $1/N$. For better visualization, we actually plot its inverse $1/(NV_{c2c})$. The dashed line demonstrates the linear scaling of the segregation time with D. The inset shows the segregation time t_s, rescaled by N^2, as a function of D.

simulations, the induction time seems to converge to about one-quarter of the segregation time for all N and $D \gtrsim 4$.

We stress that for highly confined chains, the diffusive process is only responsible for the segregation over the tiny initial separation necessary to obtain a significant effective entropic force F_{eff}. The overwhelming part of the chain "demixing" is due to directed segregation (see Fig. 2). In other words: it may take a while for the system to *start* segregating, but the segregation process itself is always governed by the effective entropic force.

Figure 6 shows the average monomer densities of the two polymers for different center-of-mass distances R_{c2c}. As predicted, the monomer densities of each chain in the overlap region are almost unaffected by the presence of a second polymer in the same space. Hence, the initial monomer density is almost twice as large as for a single chain. During segregation, the monomer densities of the individual polymers increase somewhat. In fact, the snapshots show that the polymers have very nearly separated at $R_{c2c}=48$, which is significantly less than $L_{eq}=61.1$; this demonstrates that the polymers deform during segregation: the entropic driving force is strong enough to compress the polymers. After demixing, the chains expand to their equilibrium length.
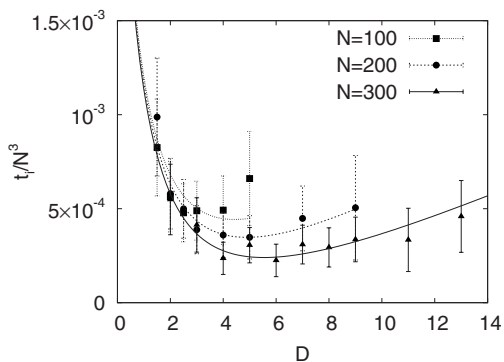

FIG. 5. Measured induction times t_i rescaled by N^3. The lines are just guides to the eye.
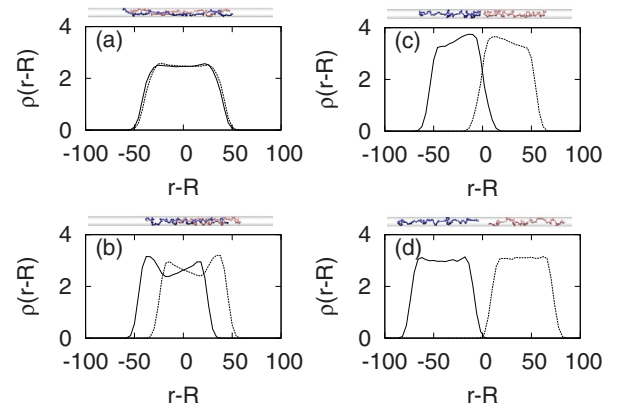

FIG. 6. (Color online) Monomer density $\rho(r)$ along the cylinder axis for $N=200$, $D=8$, averaged over all configurations with a center-of-mass distance $R_{c2c}=0$ (a), $R_{c2c}=20$ (b), $R_{c2c}=48$ (c), and $R_{c2c}=80$ (d). The graphs are centered around the systems center of mass, R.

V. CONCLUSIONS

Our simulations support the scaling prediction that the entropically driven segregation of two confined chains requires a time proportional to N^2. For long chains, this time is much shorter than the diffusive time that scales as N^3. We stress that this speed-up of entropically driven segregation does not involve any active (energy-consuming) process. Considering the geometry of confinement and the length scales of (filamenteous) bacteria, our results strongly suggest that the partitioning of duplicated chromosomes in these organisms is, at least partly, entropy driven. Since the segregation sets already in during replication, there is no initial "induction" regime for bacteria. Indeed, the recent data obtained by Hu *et al.* on the cyanobacterium *Anabaena* sp. PCC 7120 suggest that MreB, a bacterial actin homologue that is speculated by some as a "track" for transporting chromosome by putative motor proteins, is important for cell shape but not for chromosome segregation [14]. Moreover, they also have shown that the ratios of DNA content in two daughter cells have a much wider distribution than in the case that the two cells were identical. This suggests that chromosome partitioning is a random process, in good agreement with our entropy-driven segregation process we presented in this article.

[1] *Structure and Dynamics of Confined Polymers*, edited by J. J. Kasianowicz *et al.* (Kluwer Academic, Dordrecht, 2002).

[2] T. A. J. Duke, in *Multiple Aspects of DNA and RNA: From biophysics to bioinformatics*, Les Houches Session LXXXII, edited by D. Chatenay *et al.* (Elsevier, Amsterdam, 2005).

[3] B. Alberts *et al.*, *Molecular Biology of the Cell*, 4th ed. (Garland, New York, 2002).

[4] J. O. Tegenfeldt *et al.*, Proc. Natl. Acad. Sci. U.S.A. **101**, 10979 (2004).

[5] J. T. Mannion, C. H. Reccius, J. D. Cross, and H. G. Craighead, Biophys. J. **90**, 4538 (2006).

[6] T. M. Squires and S. R. Quake, Rev. Mod. Phys. **77**, 977 (2005).

[7] J. Kindt, S. Tzlil, A. Ben-Shaul, and W. M. Gelbart, Proc. Natl. Acad. Sci. U.S.A. **98**, 13671 (2001).

[8] S. Jun and B. Mulder, Proc. Natl. Acad. Sci. U.S.A. **103**, 12388 (2006).

[9] T. Cremer and C. Cremer, Nat. Rev. Genet. **292**, 1 (2001).

[10] D. Bates and N. Kleckner, Cell **121**, 899 (2005).

[11] K. Gerdes, J. Moller-Jensen, G. Ebersbach, T. Kruse, and K. Nordström, Cell **116**, 359 (2004).

[12] Z. Gitai, Cell **120**, 577 (2005).

[13] D. A. Hopwood, Annu. Rev. Genet. **40**, 1 (2006).

[14] B. Hu, G. Yang, W. Zhao, Y. Zhang, and J. Zhao, Mol. Microbiol. **63**, 1640 (2007).

[15] A. Y. Grosberg, P. G. Khalatur, and A. R. Khokhlov, Makromol. Chem., Rapid Commun. **3**, 709 (1982).

[16] S. Jun, A. Arnold, and B.-Y. Ha, Phys. Rev. Lett. **98**, 128303 (2007).

[17] J. D. Weeks, D. Chandler, and H. C. Andersen, J. Chem. Phys. **54**, 5237 (1971).

[18] H.-J. Limbach, A. Arnold, B. A. Mann, and C. Holm, Comput. Phys. Commun. **174**, 704 (2006).

[19] A. Arnold, B. Borzorgui, D. Frenkel, B.-Y. Ha, and S. Jun (unpublished).